BJPS

Brazilian Journal of
Pharmaceutical Sciences

http://dx.doi.org/10.1590/s2175-97902023e21555

Article

Applicability of [18F]FDG/PET for investigating rosmarinic acid preconditioning efficacy in a global stroke model in mice

Elaine Vasconcelos dos Santos[1], Brígida Gomes de Almeida Schirmer[1], Jousie Michel Pereira[1], Natane Vitória Silva Cardoso[1], Carlos Malamut[1*], Mércia Liane de Oliveira[2]

[1]Unidade de Pesquisa e Produção de Radiofármacos, Centro de Desenvolvimento da Tecnologia Nuclear (CDTN), Belo Horizonte, Brazil, [2]Centro Regional de Ciências Nucleares do Nordeste (CRCN-NE), Recife, Brazil

Positron emission tomography (PET) is a non-invasive nuclear imaging technique that uses radiotracers to track cell activity. The radiopharmaceutical 18F-fluoro-2-deoxyglucose ([^{18}F]FDG) is most commonly used in nuclear medicine for the diagnosis of various diseases, including stroke. A stroke is a serious condition with high mortality and morbidity rates. Rosmarinic acid (RA) is a promising therapeutic agent that exerts neuroprotective effects against various neurological diseases. Therefore, this study aimed to evaluate the applicability of [^{18}F]FDG/PET for investigating the neuroprotective effects of RA in case of a global stroke model in mice. The [^{18}F]FDG/PET technique facilitates the observation of ischemia and reperfusion injuries in the brain. Moreover, the recovery of glucose metabolism in three specific brain regions, the striatum, superior colliculus, and inferior colliculus, was observed after preconditioning with RA. It was concluded that the [^{18}F]FDG/PET technique may be useful for stroke diagnosis and the assessment of treatment response. In addition, a long-term longitudinal study using biochemical analysis in conjunction with functional imaging may provide further conclusive results regarding the effect of RA on cerebral ischemia.

Keywords: [^{18}F]FDG. Positron Emission Tomography. SUV. SPM. Rosmarinic Acid. Stroke.

INTRODUCTION

Positron emission tomography (PET) is a non-invasive nuclear imaging technique that uses radiolabeled molecular tracers with positron emitters to track cellular activity. This technique exhibits high sensitivity because it allows the detection of picomolar tracer concentrations (Vaquero, Kinahan, 2015). A commonly used radiopharmaceutical for PET imaging is 18F-fluoro-2-deoxyglucose ([^{18}F]FDG), which can detect high glucose uptake in tumors and inflammatory processes in various pathological conditions. It is used in oncology, infectious diseases, cardiac diseases, traumatology, orthopedics, endocrinology, rheumatology, psychiatry, and neurological diseases, among others (Nasrallah, Dubroff, 2013; Zhuang, Codreanu, 2015). [^{18}F]FDG/PET is useful for diagnosis, treatment planning, and predicting outcomes of various neurological diseases, including strokes.

Stroke is a serious public health problem with high mortality and disability rates, and high healthcare costs worldwide (Katan, Luft, 2018). It occurs owing to the interruption of oxygen and glucose supply to the brain because of rupture or obstruction of blood vessels, affecting homeostasis in the brain. This process results in harmful effects such as excitotoxicity, oxidative stress, inflammation, and cell death (Rodrigo *et al.*, 2013). Strokes can be hemorrhagic or ischemic, with the latter

***Correspondence:** C. Malamut. Centro de Desenvolvimento da Tecnologia Nuclear - CDTN. Seção de Pesquisa e Produção de Radiofármacos. Av. Antônio Carlos 6.627, Campus da UFMG, Pampulha. 31270-901, Belo Horizonte, Minas Gerais, Brasil. Phone: +55 31 987220370. E-mail: carlosmalamut@gmail.com / malamut@cdtn.br. ORCID: https://orcid.org/0000-0001-6405-6618

being the most common and accounting for 85–90% of cases (Katan, Luft, 2018). The treatment strategies for this condition have been extensively studied in recent decades. Revascularization using tissue plasminogen activators and endovascular thrombectomy have produced positive effects in the acute phase. However, there is no curative or preventive therapy that can halt the progressive effects of ischemia and reperfusion (Baron, 2018).

Studies on novel therapeutic approaches have reported natural compounds known as polyphenols to be promising neuroprotective agents that promote antioxidant and anti-inflammatory effects (Baron, 2018; Singh, Krishan, Shri, 2018). Rosmarinic acid (RA) is another such compound. Its beneficial effects in terms of neuroprotection, antioxidant, and anti-inflammatory effects have already been demonstrated through histological and biochemical tests as well as in vitro and in animal models (Fonteles *et al.*, 2016; Ramalho *et al.*, 2014; Zhang *et al.*, 2017).

The use of animal models to evaluate the efficacy and safety of new therapeutic approaches is widespread; however, there are limitations. For instance, the requirement of performing histological and biochemical analyses requires many animals and renders the performing of longitudinal studies impossible (Lancelot, Zimmer, 2010). Therefore, [^{18}F]FDG/PET represents a valuable resource for visualizing the effects of potential drugs in a noninvasive and optimized manner, as this technique allows the evaluation of brain function in vivo (Phelps *et al.*, 1975; Kapoor, McCook, Torok, 2004). This study aimed to evaluate the applicability of the [^{18}F]FDG/PET technique for detecting the effect of RA preconditioning in a stroke model.

MATERIAL AND METHODS

Material

[^{18}F]FDG was provided by the Nuclear Technology Development Center (Belo Horizonte, Brazil) according to standard procedures approved by the Brazilian Health Regulatory Agency ANVISA, as previously described (Ferreira *et al.*, 2009). Rosmarinic acid (RA), chemical formula C18H16O6, in powder form, with chemical purity ≥ 98% (HPLC), was purchased from Sigma-Aldrich®, USA, and 2,3,5 triphenyltetrazolium chloride (Sigma-Aldrich® (Brazil).

Animals

All experiments were performed with adult male C57Bl/6 mice aged 6–9 weeks and weighing 20-30 g, provided by the Animal Facility Center of the Federal University of Minas Gerais, Belo Horizonte, Brazil. Animals were kept under a controlled temperature environment with 12/12-h dark-light cycles and had free access to water and food. The animal care protocols adhered to the guidelines of the National Council for the Control of Experiments on Animals (CONCEA). This study was approved by the CDTN Committee on Animal Experimentation (Protocol 03/2017).

RA treatment and global ischemia model

Animals were randomly divided into four experimental groups: healthy, sham, ischemic vehicle, and RA ischemic groups. RA was dissolved in saline and administered via gavage (20 mg/kg/day, i.g.) for seven consecutive days before surgery. Saline was administered to the vehicle group. Thereafter, surgery was performed on day seven of preconditioning. The sham group underwent simulated surgery, wherein the carotid arteries were not occluded. The ischemic group underwent bilateral common carotid artery occlusion (BCCAO) with a 25-minute occlusion followed by reperfusion. Transient global cerebral ischemia was induced, as previously described by Toscano *et al.* (2016).

To detect ischemic and reperfusion injury in the brain, animals in the sham-operated, ischemic vehicle, and ischemic RA groups were euthanized by cervical dislocation 24 h after surgery, and their brains were removed and frozen in liquid nitrogen for staining with 2,3,5 triphenyltetrazolium chloride (TTC). The brain was manually cut into slices of approximately 2 mm, which were placed in 2% TTC and phosphate-buffered saline (PBS) solution, as previously described by Silva *et al.* (2015).

PET imaging and data analysis

A small-animal PET system (LabPET4 Solo, GE Healthcare Technologies, Waukesha, WI) with an axial length of 3.75 cm was used to acquire PET images and perform semiquantitative analysis (Standard Uptake Values, SUV). Two images of the animals were acquired: the first before surgery for basal or healthy group composition, and the second one day after BCCAO. Animals were under fasting for at least 6 h before imaging. After [^{18}F]FDG injection (18.7 - 23.9 MBq), the animals were kept within a slightly warmed environment and shade for 60 min before imaging to avoid excessive uptake in Harder's glands and brown fat (Jaiswal *et al.*, 2017). The animals were then anesthetized with 2% isoflurane in 100% oxygen, and static images were acquired for 30 min in a 1-bed head position. Semiquantitative values (SUV) normalized to whole-brain imaging were calculated for 14 brain regions: striatum, cortex, hippocampus, thalamus, cerebellum, basal forebrain septum, hypothalamus, amygdala, brainstem, central gray, superior colliculus, olfactory bulb, midbrain, and inferior colliculus. Thereafter, image reconstruction was performed using the maximum likelihood expectation maximization (MLEM) method in 3D with 40 iterations. A normalization file was used for the reconstruction. A phantom image was acquired to determine the calibration factor for the device. Volume-of-interest (VOI) analyses of the reconstructed images were performed using PMOD® software (version 3.3).

Statistical Parametric Mapping

To perform parametric statistical mapping, the images were preprocessed in the MATLAB environment using SPM12 software and the Small Animal Molecular Imaging Toolbox (SAMIT) tool. First, the images were realigned using rigid body registration to correct for variations owing to the position of the animal. A mouse brain model and tracer-specific [^{18}F]FDG brain template (both Ma-Benveniste mirriones) were used for image registration. Images were normalized to the injected activity and animal weight to obtain the SUV values. A mask was applied to the entire brain to avoid the influence of external recordings during the smoothing process. Further, images were smoothed with a full width at half maximum (FWHM) of 0.12 mm in all directions. In addition, an implicit mask was applied to avoid smoothing outside the defined region, whereas an explicit mask was applied for the entire brain (Ma-Benveniste-Mirrione). Subsequently, statistical analysis was performed using the two-sample Student's t-test. Consequently, results exhibiting corrected P value for FWE of less than 0.05 or the uncorrected $P < 0.0001$ were considered statistically significant.

Statistical analysis

All results were expressed as the mean ± standard deviation (SD). Student's t-test was used to compare two different groups, and one-way analysis of variance (ANOVA) was used to compare three or more groups. Statistical significance was set at a p-value of less than 0.05. Statistical analyses were performed using GraphPad Prism version 6 (GraphPad Software, Inc., San Diego, CA, USA).

RESULTS

Triphenyltetrazolium chloride (TTC) staining after BCCAO surgery

TTC staining of the brain sections was used to identify necrotic areas caused by the induction of global transient cerebral ischemia. The images demonstrated the affected regions in the ischemic groups, as indicated by the unstained regions in the brain section (Figure 1).

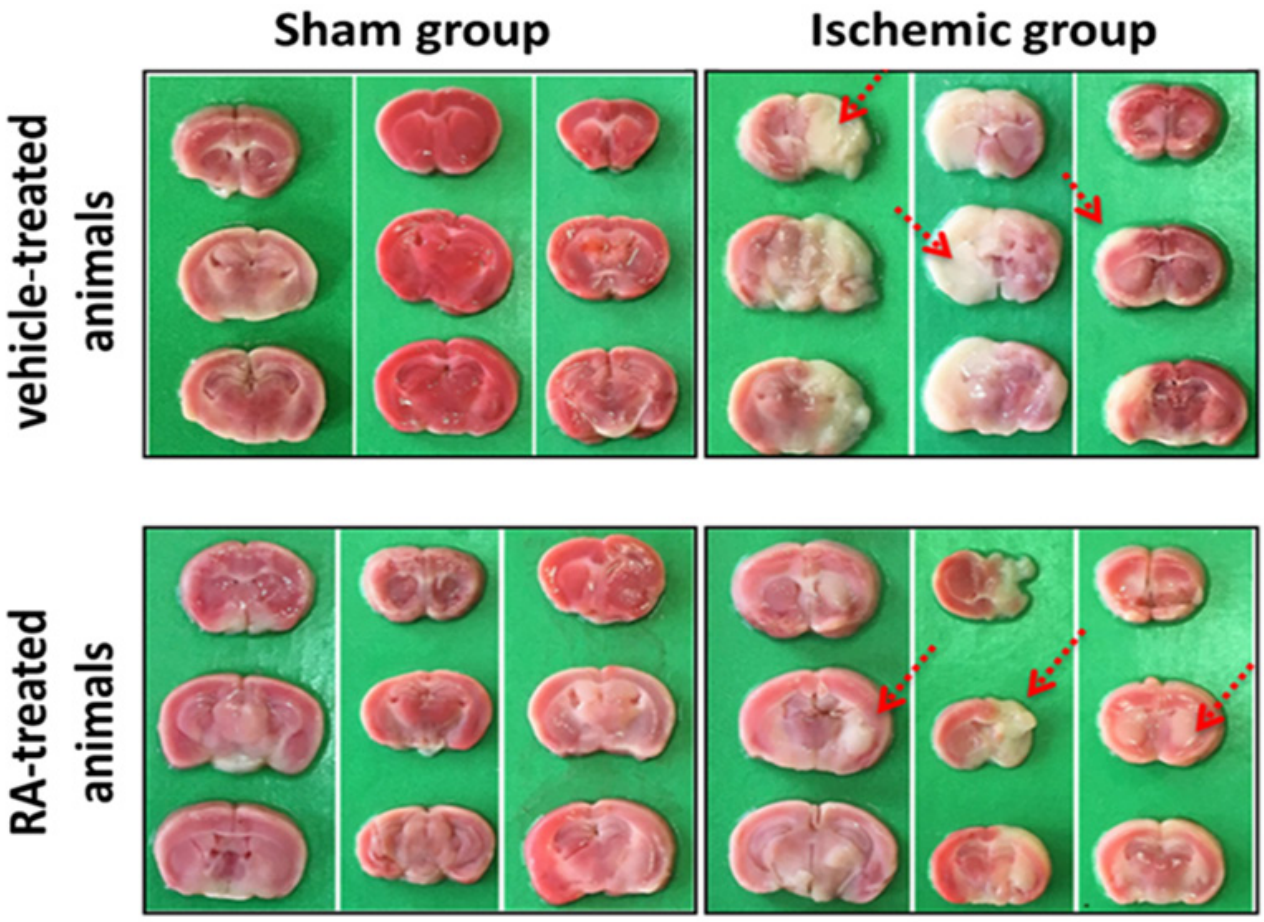

FIGURE 1 - Staining analysis of brain sections from C57BL/6 mice to identify necrotic areas. Representative images of brain sections stained with TTC from animals treated with and without RA. The red arrows show the unstained areas representing the lesion.

[18F]FDG/PET detected an improvement in the cerebral glycolytic metabolism of ischemic animals treated with RA

[^{18}F]FDG/PET images were acquired to assess the effect of RA on reduced brain metabolism in the ischemic animals (Figure 2). Semi-quantitative analysis of the PET images revealed reduced uptake in the striatum ($p = 0.0118$), superior colliculus ($p = 0.0254$), and inferior colliculus ($p = 0.0086$) in the vehicle-treated ischemic animals compared to the healthy and/or sham-treated animals. However, these regions were not affected in RA-treated animals, which exhibited the same brain metabolism in these areas as healthy animals (Figure 3). Thus, these results suggest that pre-treatment with RA has a neuroprotective effect in these animals.

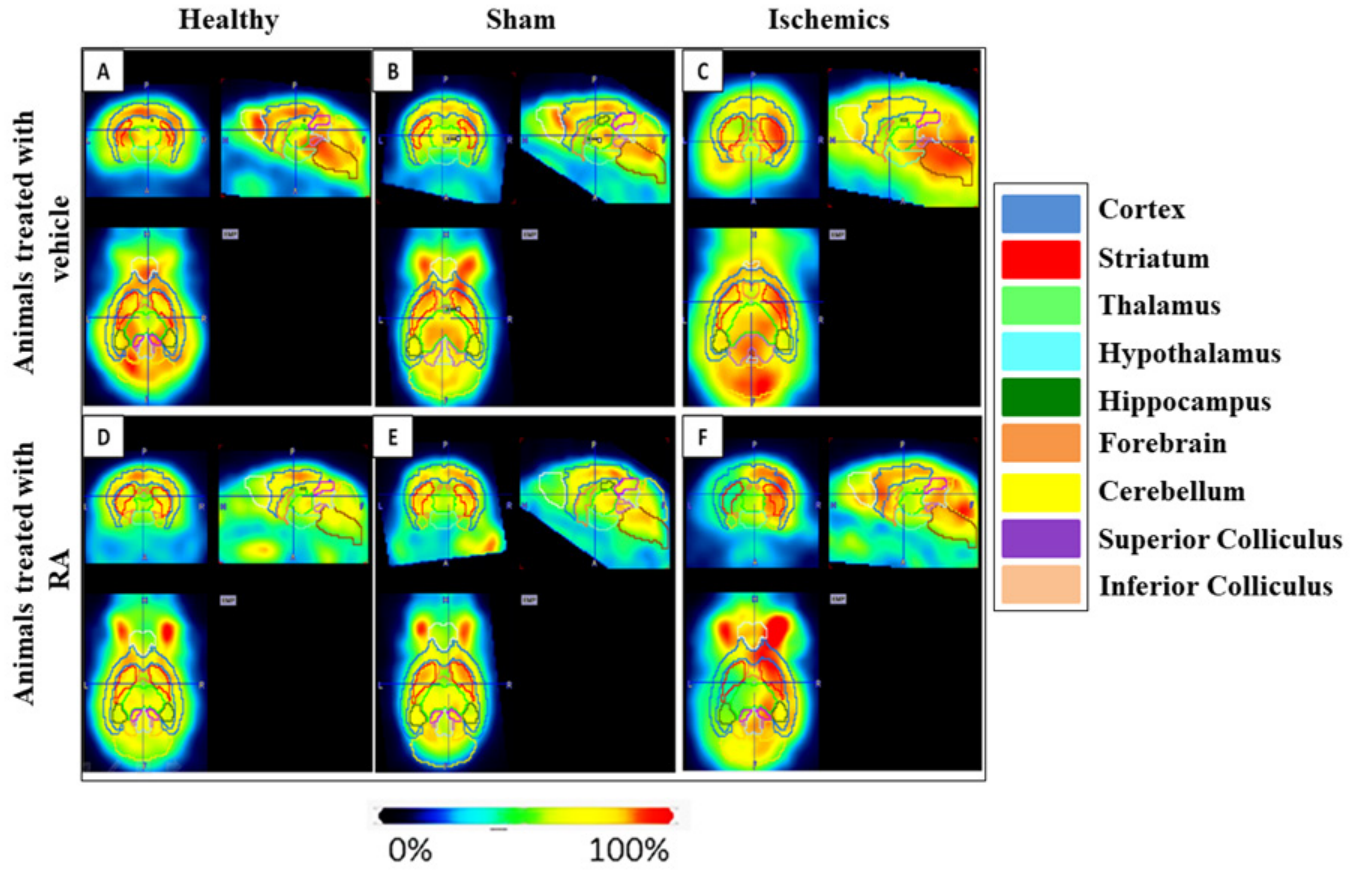

FIGURE 2 - Representative images of the uptake of [^{18}F]FDG in mouse brain mapped using PMOD software. In the figure, the most visible regions of the brain were highlighted. Vehicle-treated healthy animals (A), vehicle-treated sham animals (B), vehicle-treated ischemic animals (C), RA -treated healthy animals (D), RA -treated sham animals (E), RA -treated ischemic animals (F). Figures C and F show areas of reduced uptake of [^{18}F]FDG corresponding to regions of the cortex, striatum, hippocampus, thalamus, and superior and inferior colliculus.

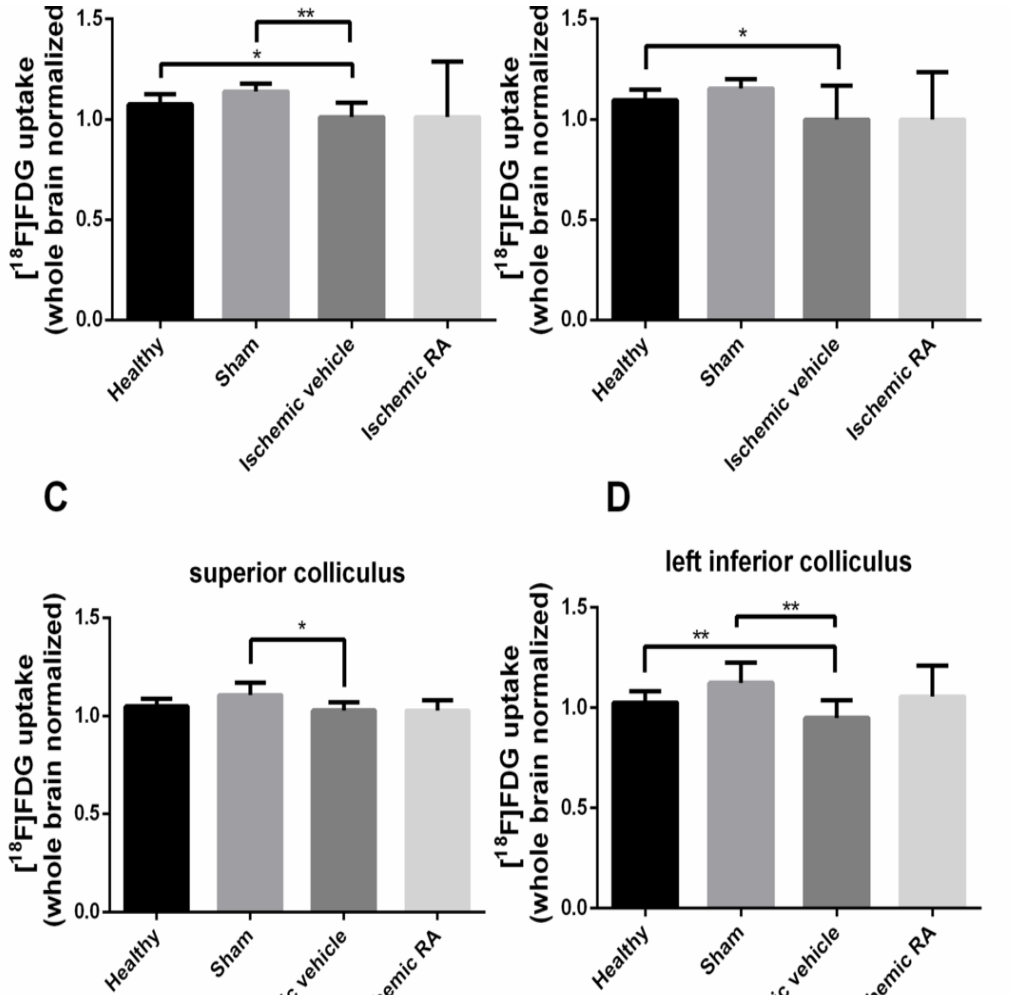

FIGURE 3 - Comparative analysis of [^{18}F]FDG uptake in the regions of the right striatum (A), left striatum (B), superior colliculus (C), and inferior colliculus (D). In these regions, the saline-treated ischemic group exhibited a lower uptake than the healthy or sham group. However, this effect was not observed in the ischemic animals treated with RA, which exhibited a similar uptake to the healthy animals. Statistical analysis was performed via Student t test using Graphpad Prism 6 software. Results are expressed as mean±standard deviation. n=24, 9, 7, and 4 for healthy, sham, vehicle-treated, and ischemic, respectively RA. ** $p < 0.005$, * $p < 0.02$.

[18F]FDG/PET detected metabolic reduction in brain regions most affected by the model

In addition, semiquantitative analysis of [^{18}F] FDG/PET revealed a reduction in uptake in the cortex ($p = 0.0068$), hippocampus ($p = 0.0078$), thalamus ($p = 0.0451$), striatum ($p = 0.0118$), superior colliculus ($p = 0.0254$), and inferior colliculus ($p = 0.0086$) regions in ischemic animals compared with healthy and/or sham-dead animals (Figures 3 and 4). This result is consistent with the regional damage profile of the model and highlights the potential diagnostic value of [^{18}F] FDG/PET in the acute phase of ischemia-reperfusion injury. Moreover, no neuroprotective effect of RA was observed in regions other than the striatum and superior and inferior colliculus. However, this effect could be demonstrated in a long-term study, for example, 3-14 days after stroke.

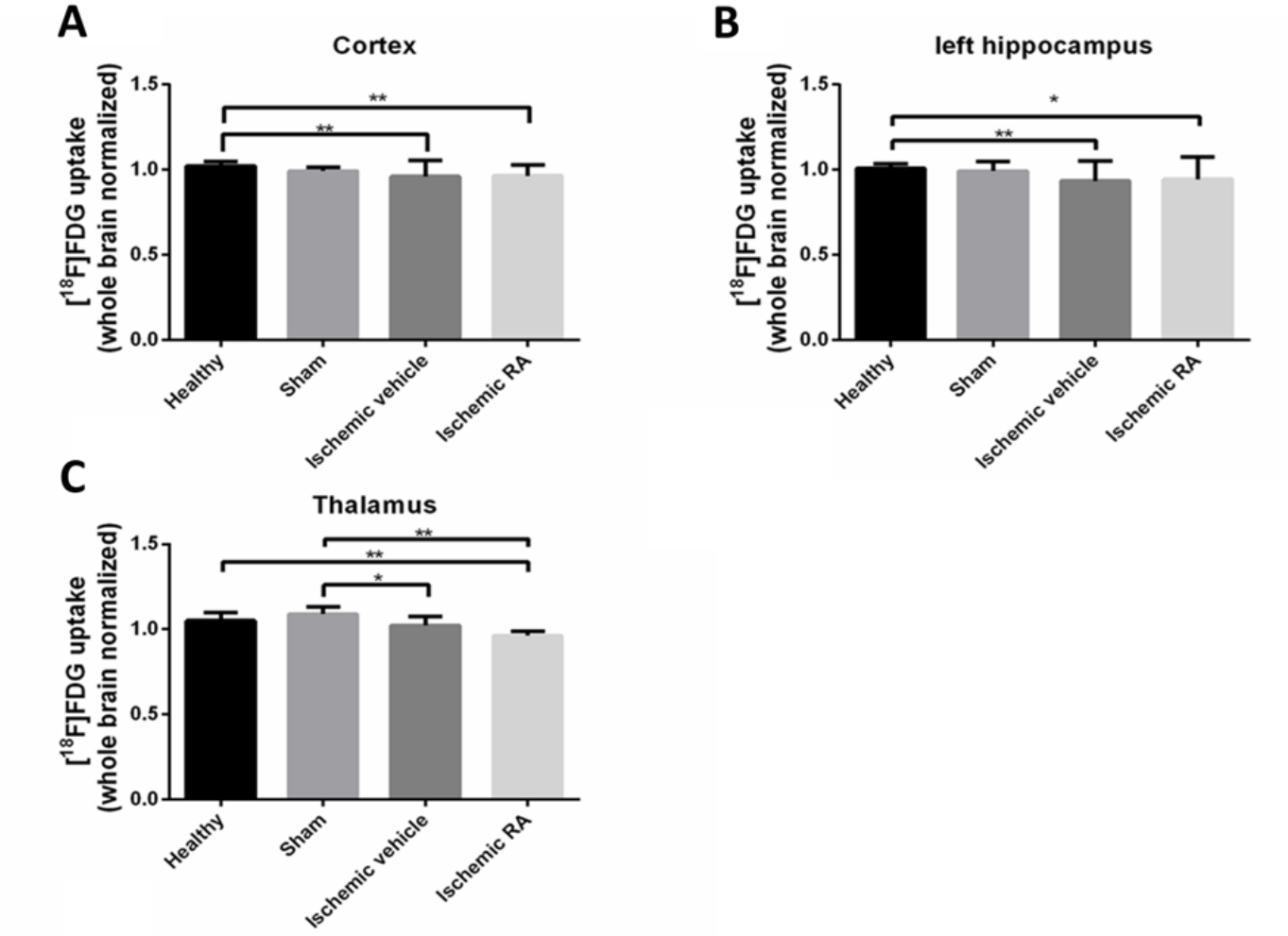

FIGURE 4 - Comparative analysis of the cortex, left hippocampus, and thalamus. Comparative analysis of [^{18}F]FDG uptake in regions of the cortex (A), left hippocampus (B), and thalamus (C). In these regions, a reduction in FDG uptake was observed in the brains of saline-treated ischemic animals compared with healthy and/or sham-treated animals. Statistical analysis was performed via Student t test using Graphpad Prism 6 software. Results are expressed as mean±standard deviation. n=24, 9, 7, and 4 for healthy, sham-ischemic, vehicle-treated, and ischemic, respectively RA. ** $p < 0.006$, * $p < 0.04$.

[18F]FDG/PET detects increased uptake in specific regions of the ischemic brain.

Of the 14 regions analyzed by [^{18}F]FDG/PET in the ischemic brain, 4 exhibited increased uptake one day after reperfusion compared to the healthy and/or sham brain: amygdala ($p = 0.0098$), brainstem ($p = 0.0003$), basal forebrain septum ($p = 0.0331$), and hypothalamus ($p = 0.0003$) (Figure 5).

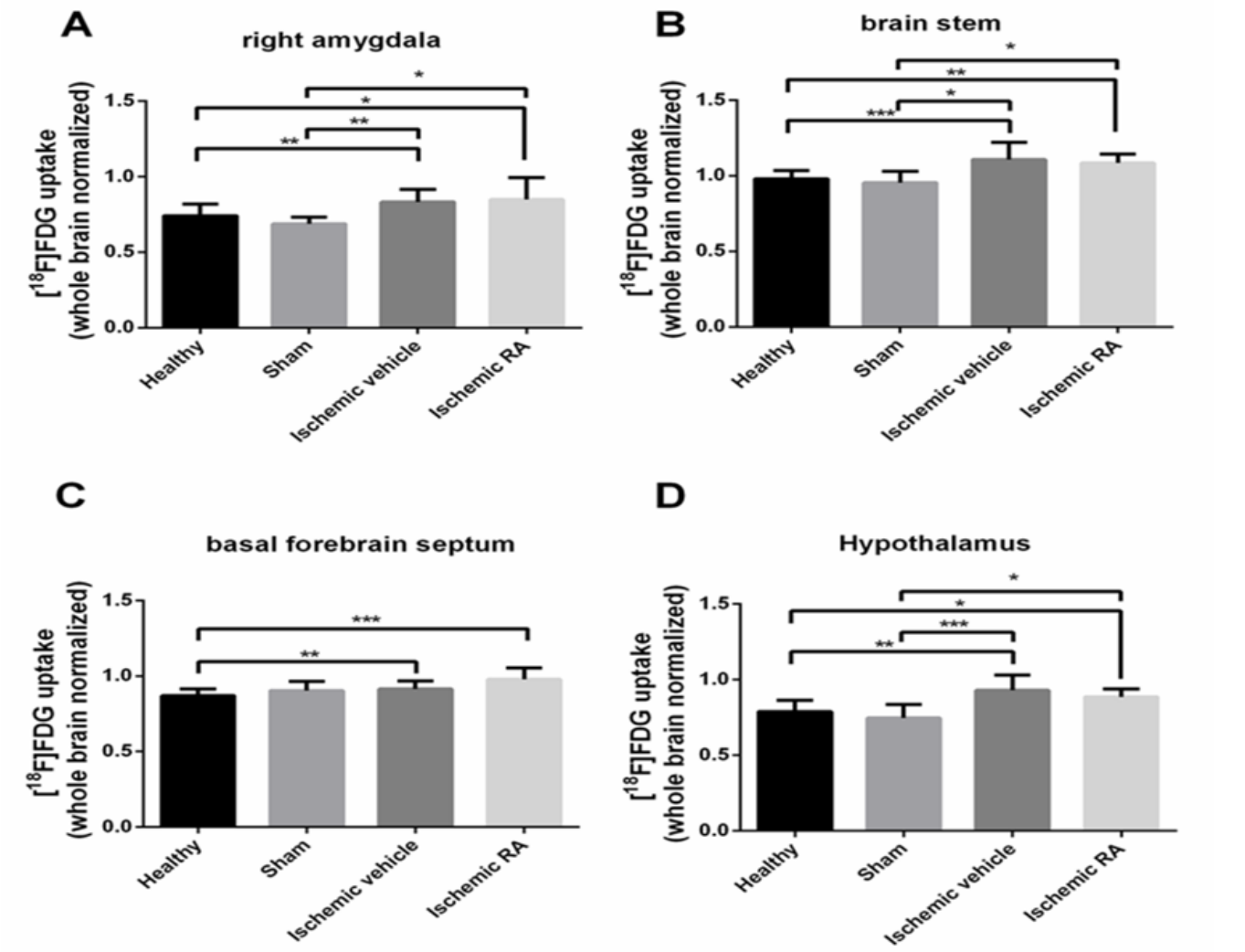

FIGURE 5 - Comparative analysis of the right amygdala, brainstem, hippocampus, forebrain septum, and hypothalamus. Comparative analysis of [^{18}F]FDG uptake in the regions of the right amygdala (A), brainstem (B), basal forebrain septum (C), and hypothalamus (D). In these regions, uptake was increased in both ischemic groups compared with the healthy or sham groups. Statistical analysis was performed via Student t test using Graphpad Prism 6 software. Results are expressed as mean±standard deviation. n=24, 9, 7, and 4 for the healthy, sham, vehicle ischemic, and ischemic groups, respectively RA. *** $p < 0.0004$, ** $p < 0.01$, * $p < 0.05$.

Effect of RA on glycolytic metabolism after brain ischemia and reperfusion - Parametric statistical mapping

For a comparison of the results of the VOI-based analysis, voxel-based analysis (statistical parametric mapping) of the [^{18}F]FDG/PET images was performed. Contrast maps of relevant statistical differences in [^{18}F]FDG uptake in the brains of the groups were generated: healthy versus ischemic vehicle and healthy versus ischemic RA. Both ischemic groups exhibited significantly reduced uptake compared to the healthy group ($p < 0.05$) (Figure 6, A and B). However, no significant difference in [^{18}F]FDG uptake was observed between the treated and untreated ischemic groups.

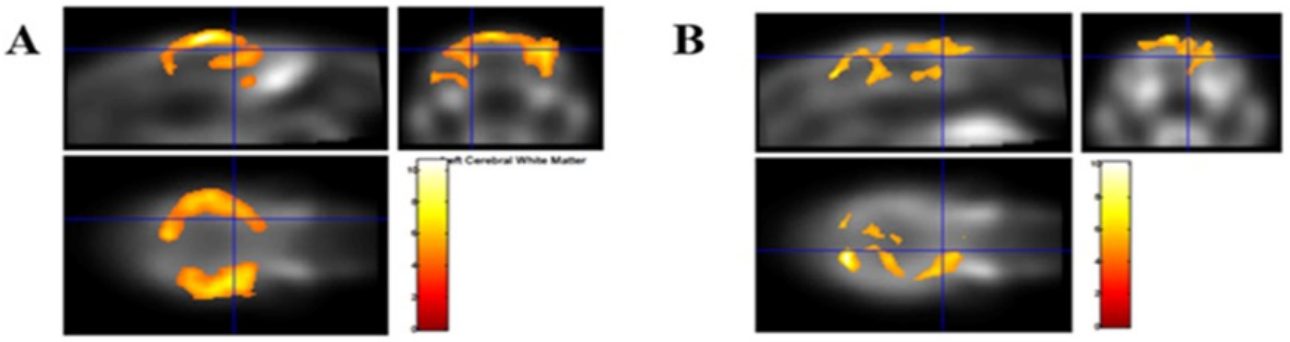

SPM analysys of [^{18}F] FDG/PET: areas with decreased metabolism of ischemic mice compared with healthy animals

Groups	Cluster		Maximum voxel					
	N°	Size (voxels)	Location			P_{FWE}	P	T
			x	y	z			
Healthy x ischemic vehicle	1	13293	-2.6	-2.0	-0.1	0.006	0.000	10.59
Healthy x ischemic RA	1	7278	1.2	-5.8	-1.3	0.126	0.000	10.11

FIGURE 6 - Statistical T maps of SPM-[^{18}F]FDG/PET analysis. Comparison between the healthy and ischemic vehicle groups (A). Comparison between healthy and ischemic RA group (B). In A, the qualitative information provided by the image in conjunction with the results shown in the Table indicate that the saline -treated ischemic group exhibited a lower uptake of [^{18}F] FDG compared with the healthy group (PFWE = 0.006). In B, ischemic animals treated with RA also exhibited a decreased uptake compared with the healthy group, but with lower intensity (P uncorrected for FWE < 0.0001). No significant differences were found in comparisons between the ischemic saline and ischemic groups RA. PFWE - p-value corrected for family-wise error; P - uncorrected p-value < 0.0001.

DISCUSSION

The pathophysiological mechanisms involved in ischemia and reperfusion injury are complex. Studies on stroke animal models, in conjunction with noninvasive molecular imaging, have facilitated investigations of the acute and chronic phases of this condition and are critical for the development of new treatments. This study showed that several analyses can identify the changes induced by the BCCAO model. The TTC staining method was used to identify necrotic areas in the brain after surgery, and [^{18}F]FDG/PET images were acquired to evaluate the metabolism and function of the brain before and after ischemia and reperfusion, with and without treatment.

Several published studies have suggested a neuroprotective effect of RA (Cui et al, 2018; Fonteles et al, 2016; Luan et al, 2013), wherein a reduction in infarct volume in ischemic mice after treatment with RA has been reported. In the first study by Cui *et al.* (2018), RA was shown to have a neuroprotective effect on memory deficits caused by a focal model of permanent ischemia (pMCAO) in mice after five days of treatment with intraperitoneal doses of 1 and 20 mg/kg/day of RA. In addition, TTC staining demonstrated that the infarcted areas were predominantly located in the ipsilateral cortex regions and, to a lesser extent, in the striatum and hippocampus. Moreover, neuronal loss was significantly lower in the treated groups than in the control. Fonteles *et al.* (2016) observed that RA suppressed the inflammatory response and astroglial activation (Fonteles *et al.*, 2016).

The [^{18}F]FDG/PET technique performed one day after reperfusion exhibited regional differences in

glycolytic metabolism in ischemic animals treated and not treated with RA. According to histological findings described in scientific studies, the regions most affected by the BCCAO model in C57BL/6 mice are the cortex, striatum, hippocampus, and thalamus (Léon-Moreno *et al.*, 2020). Similar to the results by Svoboda *et al.* (2019), those with [^{18}F]FDG/PET exhibited a decreased uptake in these four regions, in addition to the superior and inferior colliculus, in ischemic animals treated with vehicle. Such regions of hypometabolism could be observed visually in conjunction with the TTC staining results and confirmed by semiquantitative analysis based on VOIs. Further, parallel analysis based on voxels using SPM software indicated a statistically significant reduction in [^{18}F]FDG uptake in the brains of ischemic animals compared with healthy animals. These results suggest that [^{18}F]FDG/PET is efficient for diagnosing ischemia and reperfusion injury in a global stroke model.

In addition, semi-quantitative analysis with [^{18}F]FDG/PET showed that ischemic animals treated with RA did not exhibit hypometabolism in the three regions mentioned above (striatum, superior colliculus, and inferior colliculus), as was the case in vehicle-treated animals. Thus, these results confirmed the TTC staining results and reinforced the neuroprotective effect of preconditioning with RA on ischemia-reperfusion injury in the brain.

Further, it was hypothesized that the increase in [^{18}F]FDG uptake in the amygdala, brainstem, basal forebrain septum, and hypothalamus may be because of a possible compensatory mechanism. Similar results were reported by Li *et al.* (2018). In an [^{18}F]FDG/PET study of rats subjected to a focal stroke model, an increase in glycolytic metabolism was observed in the contralateral brain regions following the induced containment treatment. This effect may be a consequence of neurogenesis or the increased expression of GLUT -3. However, further studies are needed to confirm this hypothesis.

Finally, it was concluded that pretreatment with RA at a dose of 20 mg/kg/day (i.g.) had a neuroprotective effect through the reduction of the area of cerebral infarction in animals subjected to a global ischemia and reperfusion model. The [^{18}F]FDG/PET technique proved useful for detecting and distinguishing ischemia and reperfusion injury in the brain and was sufficiently sensitive to detect metabolic recovery in specific brain regions in animals treated with RA. A study with a longer duration and larger numbers of animals may provide more conclusive results regarding the effect of RA in other regions of the ischemic brain.

ACKNOWLEDGMENTS

The authors would like to thank the Foundation of Support for Science and Technology in the State of Pernambuco for financial support.

REFERENCES

Baron JC. Protecting the ischaemic penumbra as an adjunct to thrombectomy for acute stroke. Nat Rev Neurol. 2018;14(6):325–37.

Cui H-Y, Zhang X-J, Yang Y, Zhang C, Zhu C-H, Miao J-Y, et al. Rosmarinic acid elicits neuroprotection in ischemic stroke via Nrf2 and heme oxygenase 1 signaling. Neural Regen Res. 2018;13(12):2119–28.

Ferreira SZ, Silva JB, Waquil SS, Correia RF. Stability study of 2-[18F]fluoro-2-deoxy-D-glucose (18FDG) stored at room temperature by physicochemical and microbiological assays. In: 2009 International Nuclear Atlantic Conference - INAC 2009. September 27 to October 2; Rio de Janeiro: Associação Brasileira de Energia Nuclear. Available from: https://www.severin.su/wp-content/uploads/2020/01/fdg-stability.pdf

Fonteles AA, de Souza CM, de Sousa Neves JC, Menezes APF, Santos do Carmo MR, Fernandes FDP, et al. Rosmarinic acid prevents against memory deficits in ischemic mice. Behav Brain Res. 2016;297:91–103.

Jaiswal S, Cramer N, Scott J, Meyer C, Xu X, Whiting K, et al. [18F] FDG PET to study the effect of simulated high altitude on regional brain activity in mice. J Nucl Med. 2017;58(1):1246.

Kapoor V, McCook BM, Torok FS. An Introduction to PET-CT Imaging. RadioGraphics. 2004;24(2):523–43.

Katan M, Luft A. Global health neurology. Semin Neurol. 2018;38:208–11.

Lancelot S, Zimmer L. Small-animal positron emission tomography as a tool for neuropharmacology. Trends Pharmacol Sci. 2010;31(9):411–7.

León-Moreno LC, Castañeda-Arellano R, Rivas-Carrillo JD, Dueñas-Jiménez SH. Challenges and improvements

of developing an ischemia mouse model through bilateral common carotid artery occlusion. J Stroke Cerebrovasc Dis. 2020;29(5):104773

Li Y, Zhang B, Yu K, Li C, Xie H, Bao W, et al. Effects of constraint-induced movement therapy on brain glucose metabolism in a rat model of cerebral ischemia : a micro PET/CT study. Int J Neurosci. 2018; Aug;128(8):736-745.

Luan H, Kan Z, Xu Y, Lv C, Jiang W. Rosmarinic acid protects against experimental diabetes with cerebral ischemia: Relation to inflammation response. J Neuroinflammation. 2013; Feb 17;10:28.

Nasrallah I, Dubroff J. An overview of PET neuroimaging. Semin Nucl Med. 2013;43(6):449–61.

Phelps ME, Hoffman EJ, Mullani NA, Ter-Pogossian MM. Application of annihilation coincidence detection to transaxial reconstruction tomography. J Nucl Med. 1975;16(3):210–24.

Ramalho LNZ, Pasta ÂAC, Terra VA, Augusto MJ, Sanches SC, Souza-Neto FP, et al. Rosmarinic acid attenuates hepatic ischemia and reperfusion injury in rats. Food Chem Toxicol. 2014;74:270–8.

Rodrigo R, Fernández-Gajardo R, Gutiérrez R, Matamala JM, Carrasco R, Miranda-Merchak A, et al. Oxidative stress and pathophysiology of ischemic stroke: novel therapeutic opportunities. CNS Neurol Disord - Drug Targets. 2013;12(5):698–714.

Silva BC, Miranda AS de, Rodrigues FG, Silveira ALM, Resende GH de S, Moraes MFD, et al. The 5-lipoxygenase (5-LOX) inhibitor zileuton reduces inflammation and infarct size with improvement in neurological outcome following cerebral ischemia. Curr Neurovasc Res. 2015;12(4):398–403.

Singh V, Krishan P, Shri R. Improvement of memory and neurological deficit with Ocimum basilicum L. extract after ischemia reperfusion induced cerebral injury in mice. Metab Brain Dis. 2018;33(4):1111–20.

Svoboda J, Litvinec A, Kala D, Pošusta A, Vávrová L, Jiruška P, et al. Strain differences in intraluminal thread model of middle cerebral artery occlusion in rats. Physiol Res. 2019;68(1):37–48.

Toscano EC de B, Silva BC, Victoria ECG, Cardoso AC de S, Miranda AS de, Sugimoto MA, et al. Platelet-activating factor receptor (PAFR) plays a crucial role in experimental global cerebral ischemia and reperfusion. Brain Res Bull. 2016;124:55–61.

Vaquero JJ, Kinahan P. Positron emission tomography: Current challenges and opportunities for technological advances in clinical and preclinical imaging systems. Annu Rev Biomed Eng. 2015;17(1):385–414.

Zhang M, Yan H, Li S, Yang J. Rosmarinic acid protects rat hippocampal neurons from cerebral ischemia/reperfusion injury via the Akt/JNK3/caspase-3 signaling pathway. Brain Res. 2017;1657:9–15.

Zhuang H, Codreanu I. Growing applications of FDG PET-CT imaging in non-oncologic conditions. J Biomed Res. 2015;29(3):189–202.

Received for publication on 04th October 2021
Accepted for publication on 21st July 2022